

NONLINEAR OPTICAL PHENOMENA

PACS numbers: 42.55.Px; 42.60.Da; 42.65.Ky; 42.65.Lm
DOI: 10.1070/QE2013v043n09ABEH015192

Effect of nonlinear optical three-wave interaction on the lasing parameters of a dual-wavelength vertical-external-cavity surface-emitting laser

M.Yu. Morozov, Yu.A. Morozov, I.V. Krasnikova

Abstract. **The influence of nonlinear optical interaction in a semiconductor dual-wavelength vertical-external-cavity surface-emitting laser on the main parameters of dual-wavelength radiation and lasing in the long-wavelength part of the mid-IR range, obtained in this laser as a result of nonlinear wave mixing, is investigated. An increase in the pump power leads to saturation of the short-wavelength lasing intensity and to a more rapid rise in the long-wavelength lasing intensity in comparison with the linear increase in lasing intensity in these regions in the absence of nonlinear interaction. Under the conditions of nonlinear interaction, the carrier concentration in the active layers is not stabilised near the lasing threshold but changes with an increase in the pump intensity and provides the corresponding gain in the laser active region, thus maintaining steady-state lasing. Some ways for modifying the laser active region in order to obtain the most efficient lasing in the mid-IR range are proposed.**

Keywords: *mid-IR laser, semiconductor dual-wavelength laser, vertical- external-cavity surface-emitting laser, nonlinear optical frequency conversion.*

1. Introduction

An urgent problem of applied laser physics is the development of an easy-to-use semiconductor laser operating in the mid- and far-IR ranges with a sufficiently high power. Such light sources are in high demand in medicine, spectroscopy, and safety systems [1].

The development of quantum cascade lasers (QCLs) [2] became an important step in mastering the aforementioned lasing ranges. However, QCLs are characterised by a very complex structure of the active region: it contains several hundreds of quantum-confinement layers, which must be grown with a high accuracy and reproducibility. In addition, to implement cw lasing at a wavelength above 10 μm, one must apply cryogenic cooling or a strong magnetic field [3].

Another way for obtaining coherent radiation in the mid- and far-IR ranges is to apply nonlinear frequency conversion. The first experiments on generating difference-frequency radiation through nonlinear wave mixing in a nonlinear crystal were performed even in the beginning of the 1960s [4]; however, the power obtained as a result of this conversion is relatively low. The intracavity nonlinear optical interaction due to the enhancement in the wave power in the cavity is much more efficient in comparison with mixing waves from two lasers in an external nonlinear crystal [5]. Recently Scheller et al. [6] proposed to select (using a Fabry–Perot etalon) two frequencies from the gain band of a vertical-external-cavity surface-emitting laser (VECSEL). Nonlinear mixing of these two frequencies led to generation at the difference frequency in the range of 1–2 THz, with a power up to 1 mW. However, estimates showed that lasing at frequencies above 3 THz cannot be implemented in this scheme, because both mixed frequencies are chosen from the gain bandwidth of identical quantum wells (QWs).

In our opinion, a semiconductor dual-wavelength VECSEL [7] is most promising for implementing mid-IR lasing by means of intracavity nonlinear optical frequency conversion. The main difference of this laser from an ordinary VECSEL [8] is in the structure of its active region: it contains two sets of nonidentical quantum wells (QWs), designed for simultaneous lasing at two wavelengths near 1 μm, spaced by 10 to 100 nm. Thus, the difference-frequency oscillator designed on the basis of a dual-wavelength VECSEL could be an easy-to-use emitter in the wavelength range of 10–100 μm, less expensive than the existing analogues. This oscillator is also expected to have a high beam quality, because both beams formed in the laser cavity are coaxial and Gaussian (transverse-single-mode); therefore, they are completely overlapped in space. It is planned to implement intracavity nonlinear optical mixing of beams in a nonlinear periodically poled crystal characterised by quasi-phase matching (QPM) [9].

In this paper, we report the results of numerical analysis of the influence of nonlinear optical three-wave interaction on the parameters of dual-wavelength VECSEL radiation. The analysis was performed with variation in the following parameters of the system: pump power, nonlinear-crystal length, and the number of shallow and deep QWs in the active region.

2. Schematic and mathematical model of laser

Figure 1 shows a schematic of a dual-wavelength VECSEL. An active mirror, spherical mirrors M1 and M2 and output mirror M3 form a cavity in the Z configuration. Mirrors M2 and M3 have a high reflectance for the dual-wavelength laser radiation but are transparent for difference-frequency waves. Population inversion is implemented using a 808-nm diode laser.

As was mentioned above, the main difference of a dual-wavelength VECSEL from an ordinary VECSEL [8] is in the

M.Yu. Morozov, Yu.A. Morozov V.A. Kotel'nikov Institute of Radio Engineering and Electronics, Russian Academy of Sciences, Saratov Branch, ul. Zelenaya 38, 410019 Saratov, Russia;
e-mail: mikkym@mail.ru, yuri.mor@rambler.ru;
I.V. Krasnikova Yu.A. Gagarin Saratov State Technical University, ul. Politekhnicheskaya 77, 410008 Saratov, Russia;
e-mail: krasnikovaiv2012@yandex.ru

Received 27 March 2013; revision received 17 May 2013
Kvantovaya Elektronika **43** (9) 871–874 (2013)
Translated by Yu.P. Sin'kov

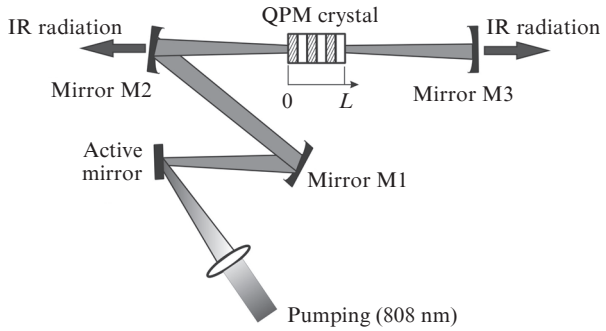

Figure 1. Schematic diagram of a dual-frequency VECSEL.

structure of the active mirror (its schematic energy-band diagram was reported in [10]). This mirror contains two sets of InGaAs QWs with different indium contents, which are designed for simultaneous amplification of dual-wavelength radiation. These QWs are separated by GaAs barrier layers, which absorb pump radiation (pumping is performed via diffusion and capture of carriers from barriers). QWs with a higher indium content (deep QWs, which are designed to emit long-wavelength radiation) are characterised by a higher capture rate and a lower carrier-escape rate in comparison with the second set of wells (shallow or short-wavelength QWs) [11]. In this context, to prevent preferred capture of carriers into deep wells, the aforementioned QW sets are separated by a wide-gap AlAs stopper, which impedes diffusion carrier transport.

The optical pumping of the active region of this laser was analysed in [12]. It was found that the concentration in all QWs of the same type can be made approximately the same. In this case, the mathematical model of the laser can be simplified: each of two sets of identical QWs can be replaced by one equivalent QW, provided that the gain of the short- and long-wavelength optical fields is preserved.

To determine steady-state lasing characteristics, we used the system of lasing rate equations [13], modified with allowance for the three-wave nonlinear optical interaction [14]:

$$\begin{aligned} &\frac{J_i}{t_w} - \frac{N_i}{\tau_r} - \frac{2}{m_i t_w}\sum_{j=1}^{2} \Gamma_{ji} g_{ji} l_j F_j \left(\frac{\omega_{ncj}}{\omega_{gj}}\right)^2 = 0, \\ &\sum_{j=1}^{2} \Gamma_{ij} g_{ij} - \alpha + \frac{1}{l_i}\ln(r_{ni} r_i) = 0. \end{aligned} \tag{1}$$

Here, the dynamic variables and parameters with the subscript $i = 1, 2$ refer to the short- and long-wavelength beams, respectively; J_i is the diffusion flux of the carriers formed by optical pumping in barrier layers to the equivalent QW of ith type; t_w is the QW width; N_i is the carrier concentration in the i_{th} QW; τ_r is the carrier lifetime in QW; m_i is the number of ith-type QWs in the active region; ω_{gj} and ω_{ncj} are the radii of the dual-wavelength beams on the active mirror and nonlinear crystal, respectively; l_i is the effective length of active mirror for the corresponding field; $\Gamma_{ij} = 2m_j t_w/l_i$ and g_{ij} are, respectively, the optical confinement factor and gain for the ith optical field in a jth quantum well; F_i is the ith-radiation photon flux; α is the wave absorption coefficient in the active mirror; and r_i is the reflectance of the ith optical field from the Bragg mirror grown in the structure.

The expression for the parameter r_{ni} (reflectance from the nonlinear element including the nonlinear crystal and mirror M3) can be written as

$$\begin{aligned} r_{n1} &= R[1 - \gamma(1 + R)F_2(0)], \\ r_{n2} &= R[1 + \gamma(1 + R)F_1(0)]. \end{aligned} \tag{2}$$

Here, R is the reflectance of mirror M3 and the factor γ characterises the efficiency of nonlinear interaction in the crystal:

$$\gamma = \frac{32Z_0}{n_1 n_2 n_3} d_{14}^2 \frac{L^2}{\lambda_1 \lambda_2} \frac{hc}{\lambda_3}, \tag{3}$$

where $\lambda_{1,2,3}$ are the lasing wavelengths (from here on, the subscript 3 denotes the difference-frequency parameters); $Z_0 = 120\pi$ is the free-space impedance; d_{14} is the element of nonlinear susceptibility tensor of the crystal; $n_{1,2,3}$ are the refractive indices of the crystal at the wavelengths $\lambda_{1,2,3}$; L is the nonlinear-crystal length; h is Planck's constant; and c is the speed of light in vacuum.

The nonlinear reflectance r_{ni} was calculated based on the formula relating the radiation photon fluxes, $F_3(L) = \gamma F_1(0)F_2(0)$ (obtained with allowance for the specific parameters of the laser under consideration from exact formulas [14] and the Manley–Rowe relations):

$$\begin{aligned} F_1(L) + F_3(L) &= F_1(0) + F_3(0), \\ F_2(L) - F_3(L) &= F_2(0) - F_3(0), \end{aligned} \tag{4}$$

where $F_{1,2,3}(0)$ and $F_{1,2,3}(L)$ are the photon fluxes at the nonlinear-crystal input and output. These formulas imply the energy conservation law at nonlinear optical interaction in the crystal (specifically, the fact that light conversion in a nonlinear crystal leads to annihilation of short-wavelength photons with simultaneous generation of long-wavelength photons; the energy released in this process is spent on emission of difference-frequency radiation).

When solving the system of equations (1), we also took into account the linear relationship between the diffusion carrier flux J_i to equivalent QWs and the pump power P_p: $J_i = K_i P_p$ (it was determined in [12], where an optical-pumping model was developed taking into account the generation of electron–hole pairs, diffusion–recombination transport to QWs, and quantum-mechanical capture in them). The lasing power P_i was determined in terms of the carrier flux F_i as $P_i = (hc/\lambda_i)F_i A_i$, where $A_i = {}^1/_2\pi\omega_{nci}^2$ $(i = 1-3)$ is the effective cross section of the Gaussian mode; note that, according to [15], the radius of the difference-frequency beam is $\omega_{nc3} = \omega_{nc1}\omega_{nc2}/(\omega_{nc1}^2 + \omega_{nc2}^2)^{1/2}$.

Since the dual-wavelength radiation is generated in laser [7] in the form of two coaxial Gaussian beams, the mathematical expression for γ [formula (3)], which is valid in the plane-wave approximation, should be replaced with

$$\gamma_G = \gamma H(\mu, \xi)/\xi \tag{5}$$

for Gaussian beams. The exact value of the focusing function $H(\mu,\xi)$ was reported in [15]. For the nonlinear-crystal lengths and beam geometric characteristics considered here, the focusing parameter ξ is rather small: $\xi = L/b \ll 1$ ($b = k_{1,2}\omega_{nc1,2}^2$ is the confocal parameter, identical for both beams,

and $k_{1,2} = 2\pi n_{1,2}/\lambda_{1,2}$ is the wave vector amplitude). In this case, the function $H(\mu,\xi)$ can be written in the simplified form:

$$H(\mu,\xi) = \frac{1-\mu}{\delta}\left[\arctan\chi - \frac{1}{2\chi}\ln(1+\chi^2)\right], \qquad (6)$$

where $\mu = k_2/k_1$; $\delta = 0.5[(1+\mu)^2 + 2(1-\mu)^2]^{1/2}$ and $\chi = 2\xi\delta/(1-\mu)$.

The thus found stationary solution to the system of equations (1), where the parameter r_{ni} was calculated from formula (2) with allowance for (3), (5), and (6), allowed us to determine the main lasing characteristics in the mid-IR range.

3. Results of simulation

Figure 2a shows the dependences of the dual-wavelength radiation power and the mid-IR lasing power at a wavelength of ~17 μm on the pump power at the following values of parameters: $\lambda_1 = 0.983$ μm; $\lambda_2 = 1.043$ μm; $\tau_r = 2$ ns; $m_1 = m_2 = 8$; $t_w = 7$ nm; $\omega_{g1,2} = \omega_{nc1,2} = 50$ μm; $\omega_{nc3} = 50/\sqrt{2} \approx 35$ μm; $l_i = 10$ μm; $\Gamma_{11} = \Gamma_{22} = 0.0112$; $\Gamma_{12} = \Gamma_{22}/10$; $\Gamma_{21} = 0$; $\alpha = 10$ cm^{-1}; $r_i = 1$; $R = 0.995$; $L = 1.4$ mm; $n_1 = 3.51$; $n_2 = 3.48$; $n_3 = 3.21$; and $d_{14} = 110$ pm V^{-1} (the nonlinear-susceptibility tensor element of GaAs was calculated according to [16]).

It can be seen in Fig. 2a that the short-wavelength power P_1 [curve (*1*)] tends to be saturated with increasing pump power, unlike the linear increase in lasing power [curves (*1′*) and (*2′*)] in the absence of nonlinear interaction. On the contrary, the long-wavelength power P_2 [curve (*2*)] increases more rapidly than in the absence of nonlinear interaction. In addition, the presence of nonlinear interaction leads to generation of difference-frequency radiation with a power P_3 [curve (*3*)], which lies in the long-wavelength part of the mid-IR range. The character of the dependences observed is explained by the energy transfer from the short-wavelength beam to the long-wavelength beam and generation of difference-frequency radiation.

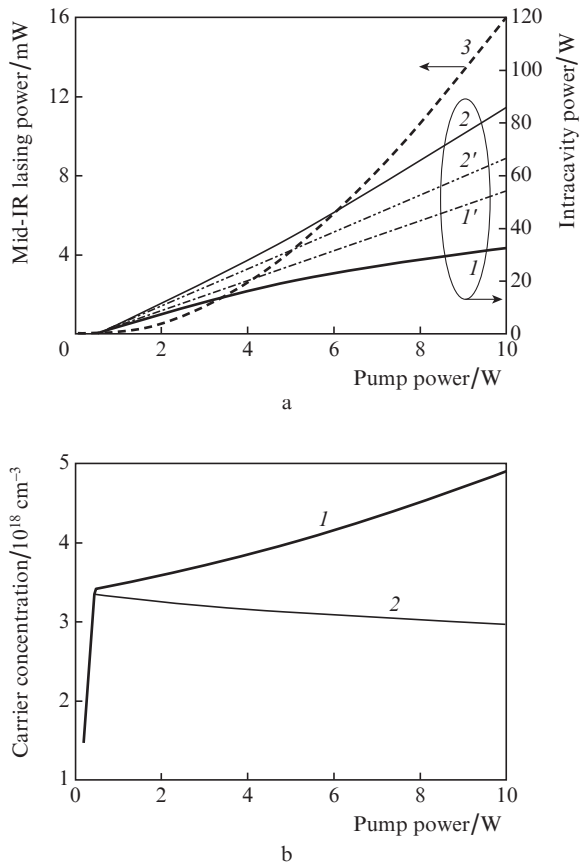

Figure 2. Dependences of the (a) short- and long-wavelength powers (*1*,*2*) in the presence and (*1′*,*2′*) in the absence of nonlinear optical interaction and (*3*) mid-IR lasing power and (b) the carrier concentration in (*1*) shallow and (*2*) deep QWs on the pump power.

The generation at the difference frequency leads to an additional loss of the short-wavelength component of dual-wavelength radiation and reduces the loss for the long-wavelength component. Hence, to maintain the lasing conditions, the short- and long-wavelength gains should be increased and decreased, respectively. The dependence of the gain on the carrier concentration for a quantum-confinement layer is logarithmic. Therefore, with an increase in the pump power, the carrier concentrations in shallow and deep QWs increase and decrease, respectively (Fig. 2b). The corresponding dependences are plotted at the same values of the parameters as in Fig. 2a.

However, when the carrier concentration in shallow QWs exceeds some critical value (~5×10^{18} cm^{-3} for the object of study: $In_{0.2}Ga_{0.8}As$ QWs with GaAs barriers), QW pumping becomes inefficient. This is due to the small difference in the carrier escape and capture times in QWs, when the number of carriers that were not captured into QWs and remained in barrier layers is sufficiently large. In this case, some part of pump power is lost in vain (specifically, it is spent on generation of electron–hole pairs remaining in the barrier layers). This inefficient loss of pumping must be excluded by limiting the carrier concentration in QWs. Therefore, it is expedient to tune the pump power so as to keep the carrier concentration below this critical value.

In Fig. 2 the numbers of shallow and deep QWs are the same: $m_{1,2} = 8$. However, with an increase in the number of shallow QWs, the short-wavelength lasing threshold will be obtained at lower carrier concentrations in these wells. Then, at a larger number of shallow QWs, the carrier concentration in them will reach the limiting level at higher pump powers or larger lengths of nonlinear crystal. Therefore, the difference-frequency lasing will be more efficient in this case.

The dependence of the mid-IR lasing power on the nonlinear-crystal length is shown in Fig. 3a. With an increase in the crystal length, the difference-frequency power increases due to the energy transfer from the short-wavelength radiation during its conversion in the crystal. As a result, to maintain the steady-state lasing conditions, the carrier concentration in shallow QWs rapidly increases and, at some value of nonlinear-crystal length (L_1 or L_2), reaches the limiting level [see Fig. 3b, curves (*1″*) and (*2″*)]. If the pump power is reduced [Fig. 3b, curves (*1′*) and (*2′*)], one can provide (beginning with the crystal length L_1 or L_2) a concentration approximately equal to the critical value (5×10^{18} cm^{-3}). Under these conditions, the mid-IR lasing power also begins to decrease; specifically this decrease explains the decline in the curves presented in Fig. 3a. We should also note that the optimal crystal length (at which the difference-frequency power reaches a maximum) depends on the number of shallow and deep QWs in the active region. Curves (*1*) and (*2*) in Fig. 3a correspond to 8 and 12 shallow QWs, respectively. The total number of wells (16) remains the same. It can be seen that, in the case of 8 shallow QWs, the optimum in the curve was observed at the crystal

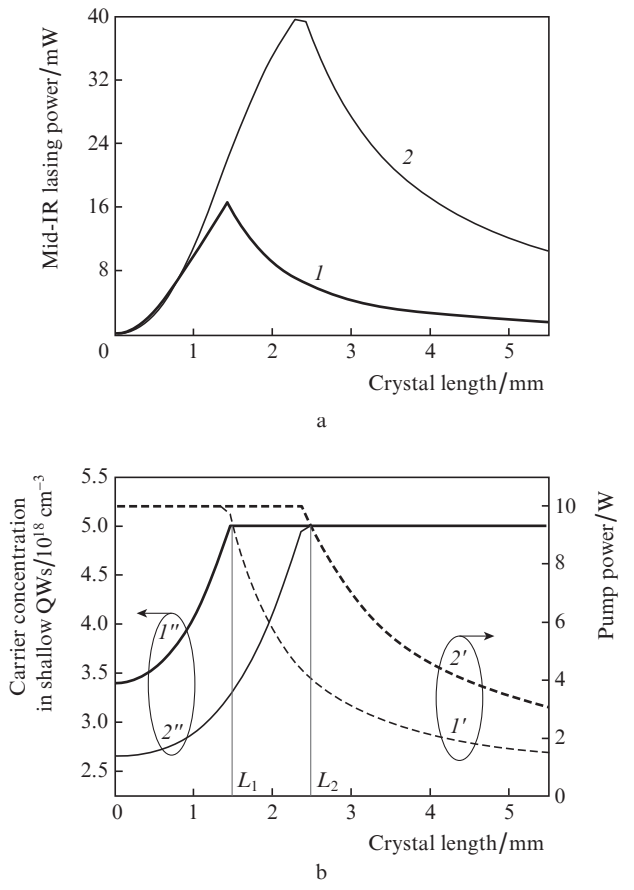

Figure 3. Dependences of the (a) difference-frequency power and (b) pump power (*1′*,*2′*) and the carrier concentration in shallow QWs (*1″*,*2″*) on the nonlinear-crystal length. The numbers of shallow QWs are (*1*,*1′*,*1″*) 8 and (*2*,*2′*,*2″*) 12; the total number of QWs is 16 in both cases.

length $L_1 \approx 1.4$ mm, while for 12 QW the corresponding length was $L_2 \approx 2.4$ mm. Therefore, the crystal length at which the nonlinear conversion in the crystal remains efficient at the maximum pump power increases with an increase in the number of shallow QWs. As a result, the maximum output mid-IR lasing power also grows with an increase in the number of shallow QWs.

4. Conclusions

Our analysis demonstrated a possibility of efficient lasing in the long-wavelength part of mid-IR range (at a wavelength of ~17 μm the maximum output power is ~40 mW for a pump power of 10 W) in a semiconductor dual-wavelength vertical-external-cavity surface-emitting laser.

The dependence of the dual-wavelength VECSEL power on the pump power upon nonlinear optical interaction was found to be highly nonlinear. Specifically, the short-wavelength power shows a tendency to saturation, while the long-wavelength power grows more rapidly than in the absence of nonlinear interaction.

It was shown that at nonlinear optical interaction the carrier concentration in QWs is not stabilised at the lasing threshold but changes during nonlinear conversion, thus providing matching between the loss and gain for dual-wavelength lasing.

To increase the difference-frequency power generated as a result of nonlinear conversion, it was proposed to form different numbers of shallow and deep QWs in the laser active region. This change in the concentration makes it possible to implement efficient nonlinear interaction at a larger number of 'short-wavelength' QWs for large crystal lengths at the maximum pump power and, correspondingly, increase the output mid-IR power.

Acknowledgements. This work was supported by the Russian Foundation for Basic Research (Grant Nos 12-02-31888-mol_a and 13-02-12070-ofi_m).

References

1. Tonouchi M. *Terahertz Sci. Technol.*, **2**, 90 (2009).
2. Beck M., Hofstetter D., Aellen T., Faist J., Oesterle U., Ilegems M., Gini E., Melchior H. *Science*, **295**, 301 (2002).
3. Wade A., Fedorov G., Smirnov D., Kumar S., Williams B.S., Hu Q., Reno J.L. *Nat. Photonics*, **3**, 41 (2009).
4. Niebuhr K.E. *Appl. Phys. Lett.*, **2**, 136 (1963).
5. Dmitriev V.G., Tarasov L.V. *Prikladnaya nelineinaya optika* (Applied Nonlinear Optics) (Moscow: Fizmatlit, 2004).
6. Scheller M., Yarborough J., Moloney J., Fallahi M., Koch M., Koch S. *Opt. Express*, **18**, 27112 (2010).
7. Leinonen T., Morozov Yu.A., Harkonen A., Pessa M. *IEEE Photonics Technol. Lett*., **17**, 2508 (2005).
8. Tropper A.C., Foreman H.D., Garnache A., Wilcox K.G., Hoogland S.H. *J. Phys. D: Appl. Phys*., **37**, 75 (2004).
9. Levi O., Pinguet T.J., Skauli T., Eyres L.A., Parameswaran K.R., Harris J.S. Jr., Fejer M.M., Kulp T.J., Bisson S.E., Gerard B., Lallier E., Becouarn L. *Opt. Lett*., **27**, 2091 (2002).
10. Morozov Yu.A., Konyukhov A.I., Kochkurov L.I., Morozov M.Yu. *Kvantovaya Elektron*., **41** (11), 1040 (2011) [*Quantum Electron*., **41** (11), 1040 (2011)].
11. Tsai C.-Y., Tsai C.-Y., Lo Y.-H., Spencer R., Eastman L. *IEEE J. Sel. Top. Quantum Electron*., **1**, 316 (1995).
12. Morozov Yu., Leinonen T., Morozov M., Ranta S., Saarinen M., Popov V., Pessa M. *New J. Phys.*, **10**, 063028 (2008).
13. Morozov M.Yu., Morozov Yu.A., Krasnikova I.V. *Radiotekh. Elektron*., **55** (10), 1243 (2010).
14. Liu X., Zhang H., Zhang M. *Opt. Express*., **10**, 83 (2002).
15. Richter D., Fried A., Weibring P. *Laser Photonics Rev.*, **3**, 343 (2009).
16. Orlov S.N., Polivanov Yu.N. *Kvantovaya Elektron*., **37** (1), 36 (2007) [*Quantum Electron*., **37** (1), 36 (2007)].